

Numerical Simulation of the Effect of Temperature- dependent Acoustic and Thermal Parameters on the Focal Temperature and Thermal Lesion of Biological Tissue Irradiated by HIFU

Hu Dong¹, Gang Liu^{1,2}, Gaofeng Peng^{1*}

1. School of Information Science and Engineering, Changsha Normal University, Changsha 410100, China
2. School of Physics and Electronics, Central South University, Changsha 410083, China

ARTICLE INFO	ABSTRACT
<p>Article type: Original Paper</p> <hr/> <p>Article history: Received: May 19, 2022 Accepted: Sep 26, 2022</p> <hr/> <p>Keywords: High-Intensity Focused Ultrasound Lesion Temperature</p>	<p>Introduction: Accurate temperature and thermal lesion prediction is very important for high-intensity focused ultrasound (HIFU) in the treatment of tumors. The traditional focal temperature and thermal lesion prediction methods usually use constant acoustic and thermal parameters. However, HIFU irradiation of biological tissue will cause its temperature rise and change the tissue characteristic parameters, which will affect the sound field and temperature field.</p> <p>Material and Methods: The constant acoustic and thermal parameters, dynamic acoustic and thermal parameters, constant acoustic and dynamic thermal parameters, dynamic acoustic and constant thermal parameters were used for simulation by Khokhlov-Zabolotskaya-Kuznetsov (KZK) equation and Pennes biological heat transfer equation (PBHTE), and their effects and differences on the focal temperature and thermal lesion of biological tissue were compared and analyzed.</p> <p>Results: The focal temperature predicted by constant acoustic parameters was less than that predicted by dynamic acoustic parameters, and the thermal lesion area predicted by constant acoustic parameters was also smaller than that predicted by dynamic acoustic parameters. On the premise of using dynamic acoustic parameters, the focal temperature predicted by dynamic thermal parameters was higher than that predicted by constant thermal parameters. When the acoustic parameters remained constant, the focal temperature predicted by dynamic thermal parameters was lower than that predicted by constant thermal parameters, but their predicted thermal lesion areas were almost the same.</p> <p>Conclusion: The temperature-dependent acoustic and thermal parameters should be considered when predicting focal temperature and thermal lesion of biological tissue, so that doctors can use the appropriate thermal dose in the surgical treatment of HIFU.</p>

► Please cite this article as:

Dong H, Liu G, Peng G. Numerical Simulation of the Effect of Temperature- dependent Acoustic and Thermal Parameters on the Focal Temperature and Thermal Lesion of Biological Tissue Irradiated by HIFU. Iran J Med Phys 2023; 20: 257-265. 10.22038/IJMP.2022.65642.2126.

Introduction

In recent years, the incidence rate and mortality of tumors have been increasing. High- intensity focused ultrasound (HIFU) can achieve non-invasive treatment of tumors and significantly improve the rehabilitation effect of patients [1,2]. In the process of HIFU treatment, the focused ultrasonic transducer uses the focusing and penetration of ultrasound to focus the low-energy ultrasound in vitro on the area requiring treatment in vivo, forming a high-energy target. The temperature of this point rises rapidly, changing the permeability and fluidity of cell membrane. Higher temperature will cause irreversible coagulation necrosis of the target tissue, but will not damage the normal tissue outside the target, so as to achieve the purpose of noninvasive treatment [3,4].

The traditional simulation of HIFU thermal ablation method sets the acoustic and thermal characteristic parameters of biological tissue as

constant parameters. However, relevant experimental studies show that HIFU irradiation of biological tissue will not only change its temperature, but also change its acoustic and thermal characteristic parameters [5-8], which will also affect the sound field and temperature field in biological tissue. Christopher et al. proposed a full three-dimensional model to study the effects of dynamic sound velocity and absorption coefficient on ultrasonic nonlinear propagation in liver tissue under HIFU irradiation, and the role of thermal lens in HIFU treatment using large focal phased array [9]. Hallaj et al. combined the acoustic temperature field and the non-uniformity of the temperature field to predict dynamic sound velocity in biological tissue, and solved the sound field in liver with and without fat layer through the acoustic thermal coupling algorithm. It was found that the size and location of lesion in liver were affected by the

*Corresponding Author: Tel: +73184036108; Email: 314644054@qq.com

thermoacoustic lens effect [10]. Guntur et al. compared the traditional method with the focal temperature predicted by thermal parameters measured at different temperature, and it was found that the traditional method significantly overestimated the focal temperature of porcine liver irradiated by HIFU [11]. As far as we know, the above research only considered the impact of dynamic acoustic and thermal parameters or thermal parameters at different temperatures on the temperature field of biological tissue. However, it is still unclear whether it is constant acoustic and thermal parameters, or dynamic acoustic and constant thermal parameters, or constant acoustic and dynamic thermal parameters, or dynamic acoustic and thermal parameters that have the most prominent impact on the temperature field. Therefore, we study the above four different combinations of acoustic and thermal parameters, and analyze the differences of temperature related acoustic and thermal parameters on focal temperature and thermal lesion of liver tissue. The research results are expected to provide medical personnel with more accurate temperature distribution and thermal lesion prediction, and have an in-depth understanding of the complex dynamic process in the process of HIFU hyperthermia, which will help doctors make treatment plans scientifically.

Materials and Methods

Numerical simulation method

The axisymmetric Khokhlov-Zabolotskaya-Kuznetsov (KZK) equation contains three terms, namely nonlinearity, diffraction, and absorption effect, which can be expressed as [12,13]:

$$\frac{\partial^2 p}{\partial z \partial t} = \frac{c}{2} \nabla_{\perp}^2 p + \frac{\delta}{2c^3} \frac{\partial^3 p}{\partial t^3} + \frac{\beta}{2\rho c^3} \frac{\partial^2 p^2}{\partial t^2} \quad (1)$$

Where P is the sound pressure, c is the sound velocity, δ is the acoustic conductivity of the medium, β is the nonlinear coefficient of the medium, $\beta = 1 + B/2A$,

ρ is the density and ∇^2 is the transverse Laplace operator [12]. In the frequency domain, the sound pressure can be expressed as [14,15]:

$$p(\xi, \sigma, \tau) = \sum_{n=1}^{\infty} \bar{p}_n(\xi, \sigma, \tau) \quad (2)$$

$\xi = z/l_d$, $l_d = \rho c^3 / \beta \omega p_0$, where z is the fundamental pressure of the transducer, ω is the fundamental angular frequency, and p_0 is the surface sound pressure of transducer. $\sigma = z/r_0$, which represents the normalized axial coordinate, and $r_0 = ka^2/2$ is the Rayleigh distance, k represents the harmonic order, and a represents the sound source radius, $\tau = \omega(t - z/c)$.

$\bar{p}_n(\xi, \sigma, \tau)$ Represents the n -order harmonic sound pressure, which is expressed as follow:

$$\bar{p}_n(\xi, \sigma, \tau) = \bar{p}_n(\xi, \sigma) \exp(-jn\tau), \quad n=1,2,\dots \quad (3)$$

Among them, in which j is the imaginary unit, the sound intensity at the focus of transducer can be expressed by each harmonic sound pressure as [16]:

$$I = \frac{1}{2\rho c} \sum_{n=1}^K |\bar{p}_n|^2 \quad (4)$$

The heating rate can be expressed as below [11,17]:

$$H = \frac{1}{\rho c} \sum_{n=1}^K |\bar{p}_n|^2 \alpha \quad (5)$$

Where α is the sound absorption coefficient. The focal temperature and thermal lesion are simulated by Pennes biological heat transfer equation (PBHTE), which can be expressed as [18,19]:

$$\rho C_t \frac{\partial T}{\partial t} = k_t \nabla^2 T + Q_v \quad (6)$$

Where C_t is the specific heat capacity, k_t is the thermal conductivity of medium, and T is the temperature of medium. Equation (6) does not consider

the heat loss caused by blood flow, and Q_v is the heat accumulation caused by sound field [20,21].

$$Q_v = 2\alpha I \quad (7)$$

The PBHTE equation is solved by finite difference time domain method (FDTD) [21].

The lesion area can be judged by the state of denaturation and ablation, which is related to the

equivalent thermal dose TD_{43} . The heat dose used to characterize the thermal lesion results is equivalent to the equivalent heating time at 43 °C. In formula (8), R is a constant. When $T \geq 43$ °C, $R = 0.5$, and when $T < 43$ °C, $R = 0.25$. The threshold of visible thermal lesion formation of biological medium is usually used at 43 °C for 240 minutes [22,23]:

$$TD_{43^\circ\text{C}} = \int_0^t R^{43-T(\tau)} d\tau \quad (8)$$

Numerical simulation model and characteristic parameters

Numerical simulation model

A two-dimensional axisymmetric geometric model of porcine liver irradiated by HIFU transducer, as shown in Figure 1. The HIFU source is concave spherical ultrasonic transducer with frequency $f = 1.0$ MHz, the geometric focal length is $F = 7.5$ cm and the half aperture is $a = 2.2$ cm. The length of porcine liver is $L = 3$ cm, and the width is $W = 1.5$ cm. The surface sound pressure of transducer is adjustable, and the excitation signal of HIFU is pulse signal with a duty cycle of 15%.

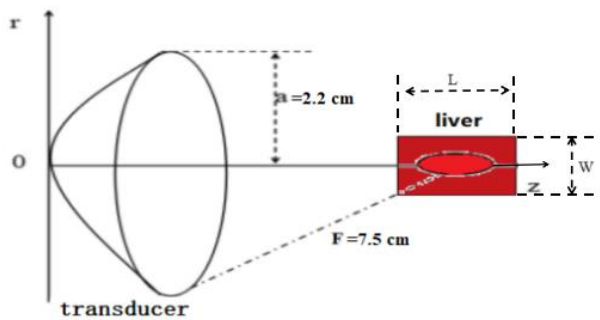


Figure 1. Geometric model of porcine liver irradiated by HIFU transducer

The transmission distance of ultrasonic wave in water is 5cm. The order of nonlinear harmonics used for simulation calculation is 128, and MATLAB R2011(MathWorks, Natick, Massachusetts, United States) software is used to simulate focal temperature and thermal lesion.

Temperature-dependent acoustic and thermal characteristic parameters

Numerous academics have carried out experimental investigations on how temperature affects the acoustic and thermal properties of porcine liver tissue. In vitro measurements of the acoustic and thermal properties of porcine liver tissue were made by Choi et al. [8, 24]. They collected information on the absorption coefficient, sound velocity, B/A, density, specific heat capacity, and thermal conductivity, where B/A is the Taylor series expansion's ratio of the second-order (B) coefficients to the first-order (A) coefficients [25]. The impact of blood perfusion rate was disregarded due to the short HIFU treatment duration, and the study's focus on the local temperature level thermal lesion of porcine liver subjected to HIFU in vitro. Due to the little modification of nonlinear B/A parameters above 75 °C with temperature rise, the features of nonlinear B/A above 75 °C are still represented by the corresponding nonlinear B/A at 75 °C in order to facilitate issue analysis [24-26]. By utilizing polynomials to fit known experimental data on the acoustic and thermal properties of porcine liver tissue, the following mathematical formulas for temperature-related acoustic and thermal parameters were created [7,8].

$$\alpha = -2.217 \times 10^{-11} \times T^7 + 9.868 \times 10^{-9} \times T^6 - 1.842 \times 10^{-6} \times T^5 + 0.0001844 \times T^4 - 0.01058 \times T^3 + 0.3481 \times T^2 - 6.189 \times T + 50.7 \quad 30^\circ\text{C} \leq T \leq 90^\circ\text{C} \quad (9)$$

$$B/A = 6.68 - 0.41448 \times T + 0.03364 \times T^2 - 0.00101 \times T^3 + 1.34407 \times 10^{-5} \times T^4 - 6.35346 \times 10^{-8} \times T^5 \quad 30^\circ\text{C} \leq T \leq 75^\circ\text{C} \quad (10)$$

$$\rho = 1084.09352 - 2.97434 \times T + 0.0042 \times T^2 + 0.00293 \times T^3 - 6.14447 \times 10^{-5} \times T^4 + 3.33019 \times 10^{-7} \times T^5 \quad 30^\circ\text{C} \leq T \leq 90^\circ\text{C} \quad (11)$$

$$c = 1529.3 + 1.6856 \times T + 6.1131 \times 10^{-2} \times T^2 - 2.2967 \times 10^{-3} \times T^3 + 2.2657 \times 10^{-5} \times T^4 - 7.1795 \times 10^{-8} \times T^5 \quad 30^\circ\text{C} \leq T \leq 90^\circ\text{C} \quad (12)$$

$$C = 3600 + 53.55552 \times T - 3.96009 \times T^2 + 0.10084 \times T^3 - 0.00106 \times T^4 + 4.01666 \times 10^{-6} \times T^5 \quad 30^\circ\text{C} \leq T \leq 90^\circ\text{C} \quad (13)$$

$$K = 0.84691 - 0.02094 \times T + 3.89971 \times 10^{-4} \times T^2 - 5.47451 \times 10^{-7} \times T^3 - 4.14455 \times 10^{-8} \times T^4 + 2.97188 \times 10^{-10} \times T^5 \quad 30^\circ\text{C} \leq T \leq 90^\circ\text{C} \quad (14)$$

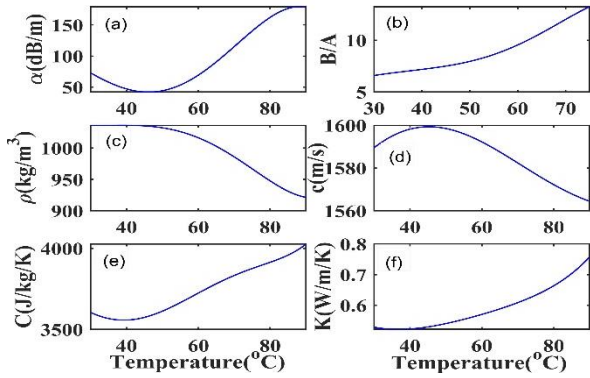


Figure 2. Temperature-dependent acoustic and thermal parameters of porcine liver tissue (a) Absorption coefficient; (b) B/A; (c) Density; (d) Sound velocity; (e) Specific heat capacity; (f) Thermal conductivity

The polynomial corresponding graph of the above fitting is shown in Figure 2. The corresponding constant acoustic and thermal parameters of porcine liver and water at 30 °C are shown in Table 1.

Table 1. Constant acoustic and thermal parameters of porcine liver and water at 30 °C [17, 18, 24]

Material properties	Units	Symbol	Porcine liver	Water
Density	kg/m ³	ρ	1036	1000
Sound velocity	m/s	c	1590	1500
Absorption coefficient	dB/m	α	70.57	0.217
B/A	/	B/A	6.6	5.0
Specific heat capacity	J/kg/K	C	3604	4180
Thermal conductivity	W/m/K	K	0.53	0.60

The irradiated area of porcine liver tissue is discretized by FDTD method, and the sound field and temperature field in the focal region are simulated and calculated in combination with KZK equation and PBHTE equation.

Results

Sound field simulation results

In HIFU sound field, the sound pressure on the transducer surface was 0.27 MPa. The effects of temperature-dependent acoustic and thermal parameters of porcine liver on nonlinear positive pressure, negative pressure, sound intensity, and heating rate were studied.

(a1) ~ (b1) with constant acoustic and thermal parameters; (a2) ~ (b2) with dynamic acoustic and thermal parameters; (a3) ~ (b3) with dynamic acoustic parameters and constant thermal parameters; (a4) ~ (b4) with constant acoustic parameters and dynamic thermal parameters

In a cycle, a single sinusoidal (or cosine) pulse ultrasonic wave has a positive and negative maximum sound pressure (i.e. peak and trough), and the in-phase focused ultrasonic transducer experience positive and negative peak sound pressure in the focus area. Due to the nonlinear propagation and focusing of ultrasound, peak positive pressure and peak negative pressure will appear in the medium [27-29], which can be calculated by equation (2). The nonlinear positive and negative pressure waveforms in porcine liver tissue were simulated and calculated by equation (2), as shown in Figure 3. The maximum peak positive pressure at the focus shown in Figure 4 (a1) ~ (a4) were 3.82 MPa, 7.01 MPa, 4.21 MPa and 3.82 MPa, respectively. The minimum peak negative pressure at the focus shown in Figure 4 (b1) ~ (b4) were -2.65 MPa, -2.58 MPa, -2.60 MPa and -2.65 MPa, respectively.

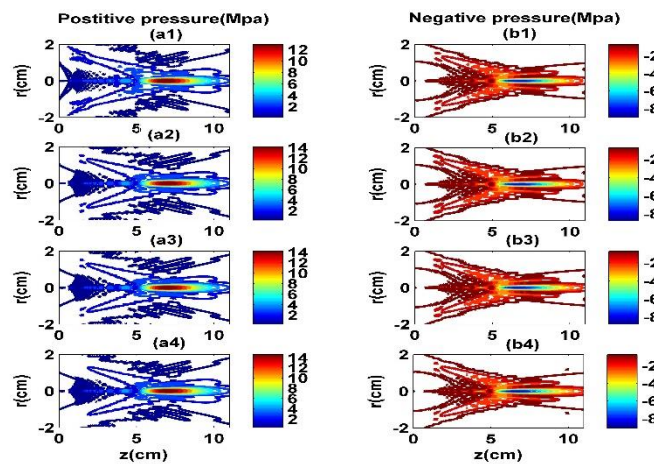


Figure 3. Simulation results of nonlinear positive pressure and negative pressure at t = 3.7 s

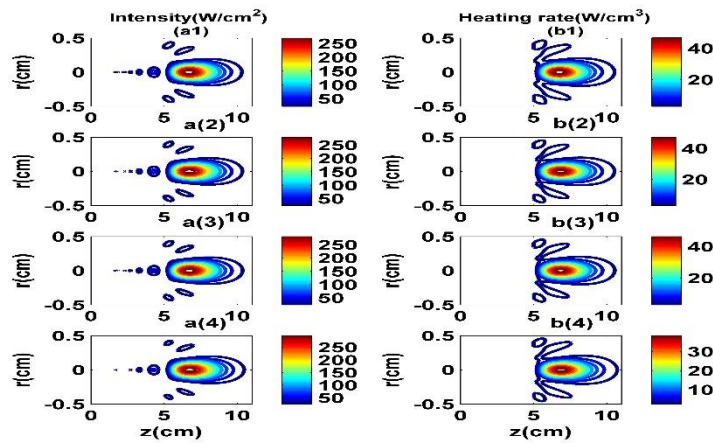


Figure 4. Simulation results of nonlinear sound intensity and heating rate at $t = 3.7$ s

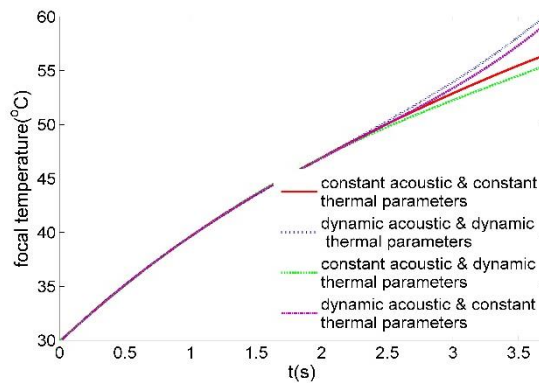


Figure 5. Effect of different temperature-dependent acoustic and thermal parameters on focal temperature of porcine liver

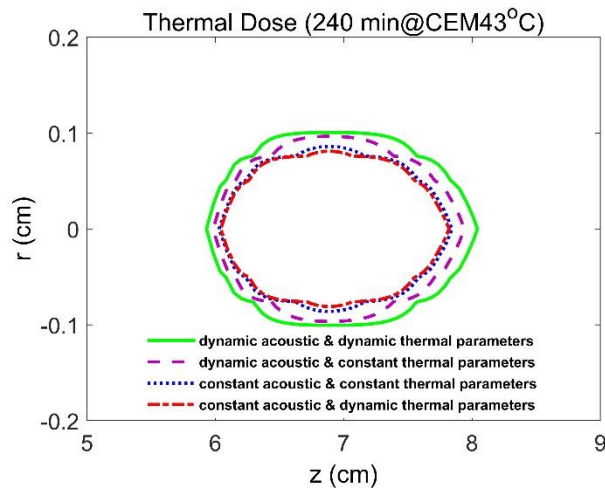


Figure 6. Comparison of effects of different temperature-dependent acoustic and thermal parameters on thermal lesion of porcine liver at $t = 3.7$ s

(a1) ~ (b1) with constant acoustic and thermal parameters; (a2) ~ (b2) with dynamic acoustic and thermal parameters; (a3) ~ (b3) with dynamic acoustic parameters and constant thermal parameters; (a4) ~ (b4) with constant acoustic parameters and dynamic thermal parameters

Figure 4 showed the above two-dimensional spatial distribution of sound intensity and heating rate simulated by equation (4) and equation (5), respectively. The

maximum sound intensity at the focus shown in Figure 4 (a1) ~ (a4) were 292.2 W/cm^2 , 303.0 W/cm^2 , 306.9 W/cm^2 and 292.2 W/cm^2 , respectively. The maximum heating rate at the focus shown in Figure 4 (b1) ~ (b4) were 43.43 W/cm^3 , 51.26 W/cm^3 , 49.27 W/cm^3 and 43.43 W/cm^3 , respectively.

Temperature field simulation results

Dynamic acoustic and thermal parameters, dynamic acoustic and constant thermal parameters, constant acoustic and dynamic thermal parameters were used to simulate the changes of focal temperature and thermal lesion of porcine liver tissue irradiated by HIFU. The corresponding dynamic acoustic and thermal parameters were updated every 0.1 s.

Figure 5 showed the focal temperature change simulation using constant acoustic and thermal parameters, dynamic acoustic and thermal parameters, constant acoustic and dynamic thermal parameters, dynamic acoustic and constant thermal parameters, respectively. Before HIFU irradiation for 2.4 s, using the above four different combinations of acoustic and thermal parameters for simulation, the focal temperature rise rate is almost the same.

After HIFU irradiation for 2.4 s, the focal temperature rising rate simulated by dynamic acoustic and thermal parameters was the fastest, followed by the temperature rising rate simulated by dynamic acoustic and constant thermal parameters and constant acoustic and thermal parameters, respectively, while the focal temperature rising rate simulated by constant acoustic and dynamic thermal parameters was the slowest.

When the irradiation time was 3.7 s, the focal temperature of simulation using constant acoustic and thermal parameters, dynamic acoustic and thermal parameters, constant acoustic and dynamic thermal parameters, dynamic acoustic and constant thermal parameters were 59.99 °C, 59.17 °C, 56.43 °C and 55.45 °C, respectively.

In Figure 6, dynamic acoustic and thermal parameters, dynamic acoustic and constant thermal parameters, constant acoustic and thermal parameters, constant acoustic and dynamic thermal parameters were used for thermal lesion simulation. The elliptical thermal lesion areas were $2.09 \times 0.20 \text{ cm}^2$, $1.98 \times 0.18 \text{ cm}^2$, $1.80 \times 0.15 \text{ cm}^2$ and $1.80 \times 0.14 \text{ cm}^2$, respectively. These phenomena showed that the thermal lesion area predicted by constant acoustic parameters was smaller than that predicted by dynamic acoustic parameters. However, when the acoustic parameters remain constant, the difference between the thermal lesion area predicted by constant thermal parameters and dynamic thermal parameters was very small.

Discussion

Generally speaking, compared with the focal temperature or thermal lesion predicted by dynamic acoustic parameters, the focal temperature or thermal lesion area predicted by constant acoustic parameters was smaller. Therefore, dynamic acoustic parameters had the most important influence on the focal temperature and thermal lesion area, and the influence was more obvious with the increase of HIFU irradiation time. Compared with other parameters, the absorption coefficient in the acoustic parameters had the greatest impact on the thermal lesion [30], because according to

the calculation of equation (7), the larger the absorption coefficient, the larger the Q_v value, the higher the focal temperature, and thus the larger the thermal lesion area. Meanwhile, although the dynamic acoustic parameters had the greatest influence on the focal temperature and thermal lesion area, the influence of other dynamic thermal parameters on HIFU heating could not be ignored.

Soon after HIFU irradiation, the predicted focal temperature of both constant and dynamic acoustic parameters was almost the same. This may be due to the small change of sound absorption coefficient of liver tissue in the early stage of HIFU irradiation [30]. It can be seen from Figure 2 (a) that the sound absorption coefficient of liver tissue changed slightly from 30 °C to 50 °C, but after 50 °C, the sound absorption coefficient of liver tissue gradually increased. After HIFU irradiation for a period of time, it was worth mentioning that under the condition that the acoustic parameters remained constant, the rising rate of focal temperature predicted using dynamic thermal parameters was slower than that predicted using constant thermal parameters, which indicated that due to the local changes of liver tissue characteristic parameters near the acoustic focus, the dynamic thermal parameters had little effect on the temperature during HIFU heating. It can be seen from Figure 2 (e) and (f) that when the temperature of liver tissue exceeded 50 °C, its specific heat capacity and thermal conductivity gradually increased. This phenomenon can be explained by the physical meaning of specific heat capacity, which was defined as the heat required to increase the temperature of unit mass tissue by 1 °C [31]. For the same amount of heat and mass, the greater the specific heat capacity, the smaller the temperature rise. In addition, due to thermal diffusion, the greater the thermal conductivity, the more heat energy was lost [32,33]. Therefore, the greater the thermal conductivity, the slower the focal temperature rising, which was similar to Guntur's research results [11]. In the clinical treatment of HIFU, due to the influence of dynamic acoustic and thermal parameters and thermal diffusion, there may be closed areas connected by multiple lesion area, which were also affected by ultrasonic intensity, moving distance of ultrasonic transducer and heating time [34], but too large lesion area would lead to over treatment and lesion to surrounding normal tissue. However, the dynamic thermal parameters and constant thermal parameters predict the thermal lesion area almost the same. It was mainly because the size of the thermal lesion area depended on the thermal dose at 43 °C for more than 240 minutes, which was the commonly accepted threshold value for cell death to occur [35,36], rather than the focal temperature.

Among various combinations of acoustic and thermal parameters, dynamic acoustic and thermal parameters had the greatest influence on temperature and thermal lesion area, which was similar to the research results of Tan and Zou [30,34], but they did not

study the effects of dynamic acoustic and constant thermal parameters, constant acoustic and dynamic thermal parameters on focal temperature and thermal lesion. Hallaj et al. studied the thermo-acoustic lens effect and used dynamic acoustic parameters to simulate the thermal lesion of liver tissue irradiated by HIFU, but they did not consider the influence of dynamic thermal parameters on thermal lesion [10]. Dong et al. studied the effects of acoustic and thermal characteristic parameters of liver tissue at different temperature on thermal lesions, but this study only focused on the acoustic and thermal characteristic parameters at specific temperature, rather than dynamic acoustic and thermal characteristic parameters [37]. Understanding the influence of the combination of various acoustic and thermal parameters on the temperature and thermal lesion area was conducive to our deep understanding of the treatment principle of HIFU. The results showed that compared with the focal temperature and thermal lesion area predicted by constant acoustic and thermal parameters, the focal temperature and thermal lesion area predicted by dynamic acoustic and thermal parameters increased, which meant that compared with the simulation using all dynamic tissue characteristic parameters, the traditional simulation method using constant acoustic and thermal parameters underestimated the focal temperature and thermal lesion area.

Conclusion

In this paper, the effects of temperature-dependent acoustic and thermal parameters of porcine liver tissue on focal temperature and thermal lesion were studied through simulation. The differences of focal temperature and thermal lesion obtained by simulation with constant acoustic and thermal parameters, dynamic acoustic and thermal parameters, constant acoustic and dynamic thermal parameters, dynamic acoustic and constant thermal parameters are compared respectively. Therefore, when doctors use HIFU equipment to treat tumor tissue, it is necessary to consider the actual impact of temperature-dependent acoustic and thermal parameters on the focal temperature and thermal lesion area, and formulate a more accurate clinical treatment plan, so as to avoid accidental lesion to the normal tissue around tumor tissue. Two areas of future study will be the main focus: First, setting up experimental circumstances and carrying out experimental research to validate simulation findings. Second, the same tests and simulations will be performed in the future if experimental data on the acoustic and thermal characteristic parameters of other organs at various temperatures are available.

Acknowledgment

This work was supported by the Key Project of Hunan Provincial Department of Education of China under grant No. 21A0618, Changsha Natural Science Foundation Project under grant No. kq2202313. The authors sincerely thank the anonymous reviewers for their helpful comments and suggestions.

References

1. Torres-de la Roche LA, Rafiq S, Devassy R, Verhoeven HC, Becker S, De Wilde R. Should Ultrasound-Guided High Frequency Focused Ultrasound Be Considered as an Alternative Non-Surgical Treatment of Uterine Fibroids in Non-Asiatic Countries? An Opinion Paper. *Journal of Clinical Medicine*. 2022;11(3): 839. DOI:10.3390/jcm11030839.
2. Wong F, Wong PH, Li T KT .How to Avoid Medico-Legal Litigations in Performing High Intensity Focused Ultrasound Ablation for Treating Fibroids and Adenomyosis. *Clinical and Experimental Obstetrics & Gynecology*. 2023; 50(1):18. DOI:10.31083/j.ceog5001018.
3. Díaz-Alejo, Jesús Frutos, Iciar Gonzalez Gomez, Julie Earl. Ultrasounds in cancer therapy: A summary of their use and unexplored potential. *Oncology Reviews*. 2022;16(1):531. DOI:10.4081/oncol.2022.531.
4. Cindric H, Gasljevic G, Edhemovic I, Breclj E, Zmuc J, Cemazar M, Seliskar A, Miklavcic D, Kos B. Numerical mesoscale tissue model of electrochemotherapy in liver based on histological findings. *Scientific Reports*. 2022 Apr 20;12(1):6476. DOI: 10.1038/s41598-022-10426-2.
5. Lin CK, Oehm L, Liebler M, Brehm H, Jenderka KV, Majschak JP. Heating of Polymer Films Induced by HIFU: Study of Acoustic and Thermal Effects. *IEEE Transactions on Ultrasonics, Ferroelectrics, and Frequency Control*. 2019 Sep 11;67(6):1201-9. DOI:10.1109/TUFFC.2019.2940380.
6. Mohammadpour M, Firoozabadi B. High intensity focused ultrasound (HIFU) ablation of porous liver: Numerical analysis of heat transfer and hemodynamics[J]. *Applied Thermal Engineering*. 2020; 170:115014. DOI: 10.1016/j.applthermaleng.2020.115014.
7. Xin Y, Zhang A, Xu LX, Fowlkes JB. Numerical study of bubble cloud and thermal lesion evolution during acoustic droplet vaporization enhanced HIFU treatment. *Journal of Biomechanical Engineering*. 2022 Mar 1;144(3):031007. DOI:10.1115/1.4052374.
8. Namakshenas P, Mojra A. Microstructure-based non-Fourier heat transfer modeling of HIFU treatment for thyroid cancer. *Computer Methods and Programs in Biomedicine*. 2020; 197:105698. DOI:10.1016/j.cmpb.2020.105698.
9. Christopher T. HIFU focusing efficiency and a twin annular array source for prostate treatment. *IEEE Transactions on Ultrasonics Ferroelectrics & Frequency Control*. 2005; 52(9):1523-33. DOI:10.1109/tuffc.2005.1516025.
10. Zhao P, Wang Y, Tong S, Tao J, Sheng Y. The Effects of Energy on the Relationship between the Acoustic Focal Region and Biological Focal Region during Low-Power Cumulative HIFU Ablation. *Applied Sciences*. 2023 Apr 1;13(7):4492. DOI:10.3390/app13074492.
11. Guntur SR, Choi MJ. Influence of Temperature-Dependent Thermal Parameters on Temperature Elevation of Tissue Exposed to High-Intensity Focused Ultrasound: Numerical Simulation. *Ultrasound in Medicine & Biology*. 2015;

- 41(3):806-13.
DOI:10.1016/j.ultrasmedbio.2014.10.008.
12. Liu S, Yang Y, Li C, Guo X, Tu J, Zhang D. Prediction of HIFU propagation in a dispersive medium via khokhlov – Zabolotskaya – Kuznetsov model combined with a fractional order derivative. *Applied Sciences*. 2018 Apr 12;8(4):609. DOI:10.3390/app8040609.
 13. Kagami S, Kanagawa T, Ayukai T. Theoretical Improvement of a KZK equation for focused ultrasound in bubbly liquids with thermal effects. *The Journal of the Acoustical Society of America*. 2020; 148(4):2572. DOI:10.1121/1.5147139.
 14. Yuldashev PV, Karzova MM, Kreider W, Rosnitskiy PB, Sapozhnikov OA, Khokhlova VA. " HIFU Beam: " A Simulator for Predicting Axially Symmetric Nonlinear Acoustic Fields Generated by Focused Transducers in a Layered Medium. *IEEE transactions on ultrasonics, ferroelectrics, and frequency control*. 2021 Apr 20;68(9):2837-52. DOI: 10.1109/TUFFC.2021.3074611.
 15. Wear KA, Shah A, Baker C. Spatiotemporal deconvolution of hydrophone response for linear and nonlinear beams—Part II: Experimental validation. *IEEE transactions on ultrasonics, ferroelectrics, and frequency control*. 2022 Feb 10;69(4):1257-67. DOI: 10.1109/TUFFC.2022.3150179.
 16. Yoon K, Lee W, Lee JE, Xu L, Croce P, Foley L, et al. Effects of sonication parameters on transcranial focused ultrasound brain stimulation in an ovine model. *PloS one*. 2019 Oct 24;14(10):e0224311. DOI:10.1371/journal.pone.0224311.
 17. Sojahrood AJ, Earl R, Haghi H, Li Q, Porter TM, Kolios MC, et al. Nonlinear dynamics of acoustic bubbles excited by their pressure-dependent subharmonic resonance frequency: influence of the pressure amplitude, frequency, encapsulation and multiple bubble interactions on oversaturation and enhancement of the subharmonic signal. *Nonlinear Dynamics*. 2021 Jan;103:429-66. DOI:10.1007/s11071-020-06163-8.
 18. Zhou Y, Yu Z, Ma Q, Guo G, Tu J, Zhang D. Noninvasive treatment-efficacy evaluation for HIFU therapy based on magneto-acousto-electrical tomography. *IEEE Transactions on Biomedical Engineering*. 2018 Jul 6;66(3):666-74. DOI:10.1109/TBME.2018.2853594.
 19. Bing C, Cheng B, Staruch RM, Nofiele J, Wodzak Staruch M, Szczepanski D, et al. Breath-hold MR-HIFU hyperthermia: phantom and in vivo feasibility. *International Journal of Hyperthermia*. 2019 Jan 1;36(1):1083-96. DOI:10.1080/02656736.2019.1679893.
 20. Yang D, Ni Z, Yang Y, Xu G, Tu J, Guo X, et al. The enhanced HIFU-induced thermal effect via magnetic ultrasound contrast agent microbubbles. *Ultrasonics sonochemistry*. 2018 Dec 1;49:111-7. DOI:10.1016/j.ultsonch.2018.07.031.
 21. Chang N, Lu S, Qin D, Xu T, Han M, Wang S, Wan M. Efficient and controllable thermal ablation induced by short-pulsed HIFU sequence assisted with perfluorohexane nanodroplets. *Ultrasonics Sonochemistry*. 2018 Jul 1;45:57-64. DOI:10.1016/j.ultsonch.2018.02.033.
 22. Abbass MA, Killin JK, Mahalingam N, Hooi FM, Barthe PG, Mast TD. Real-time spatiotemporal control of high-intensity focused ultrasound thermal ablation using echo decorrelation imaging in ex vivo bovine liver. *Ultrasound in medicine & biology*. 2018 Jan 1;44(1):199-213. DOI:10.1016/j.ultrasmedbio.2017.09.007.
 23. Raymond JL, Cleveland RO, Roy RA. HIFU-induced changes in optical scattering and absorption of tissue over nine orders of thermal dose. *Physics in Medicine and Biology*. 2018;63. DOI:10.1088/1361-6560/aaed69.
 24. Choi MJ, Guntur SR, Lee JM, Paeng DG, Lee KI, Coleman A. Changes in ultrasonic properties of liver tissue in vitro during heating-cooling cycle concomitant with thermal coagulation. *Ultrasound in medicine & biology*. 2011 Dec 1;37(12):2000-12.
 25. Sarkar R, Kumar Pandey P, Kundu S, Panigrahi PK. Exact sub and supersonic pressure wave-fronts in nonlinear thermofluid medium. *Waves in Random and Complex Media*. 2021 Jul 23:1-4. DOI:10.1080/17455030.2021.1954263.
 26. Dong H, Liu G, Tong X. Influence of temperature-dependent acoustic and thermal parameters and nonlinear harmonics on the prediction of thermal lesion under HIFU ablation. *Math. Biosci. Eng*. 2021 Jan 1;18:1340-51. DOI:10.3934/mbe.2021070.
 27. Horiba T, Ogasawara T, Takahira H. Cavitation inception pressure and bubble cloud formation by backscattering from bubble interfaces in HIFU. *21st International Symposium on Nonlinear Acoustics*. 2018;34:045041. DOI: 10.1121/2.0000919.
 28. EM Ponomarchuk, C Hunter, M Song, et al. Mechanical damage thresholds for hematomas near gas-containing bodies in pulsed HIFU fields. *Physics in Medicine & Biology*. 2022; 67(21): 215007. DOI 10.1088/1361-6560/ac96c7.
 29. Pahk KJ. Control of the dynamics of a boiling vapour bubble using pressure-modulated high intensity focused ultrasound without the shock scattering effect: A first proof-of-concept study. *Ultrasonics Sonochemistry*. 2021 Sep 1;77:105699. DOI:10.1016/j.ultsonch.2021.105699.
 30. Tan Q, Zou X, Ding Y, Zhao X, Qian S. The influence of dynamic tissue properties on HIFU hyperthermia: A numerical simulation study. *Applied Sciences*. 2018 Oct 16;8(10):1933. DOI:10.3390/app8101933.
 31. Andreozzi A, Brunese L, Iasiello M, Tucci C, Vanoli GP. Variable porosity-based bioheat model vs variable perfusion-based Pennes' equation: A comparison with in vivo experimental data. *Thermal Science and Engineering Progress*. 2022 Oct 1;35:101469. DOI: 10.1016/j.tsep.2022.101469.
 32. Mohammed BN, Ismael DS. A Computational Model for Temperature Monitoring During Human Liver Treatment by Nd: Yag Laser Interstitial Thermal Therapy (LITT). *Aro-The Scientific Journal Of Koya University*. 2022;10(2):38-44. DOI:10.14500/aro.10949.
 33. Haddadi S, Ahmadian MT. Analysis of nonlinear acoustic wave propagation in HIFU treatment using Westervelt equation. *Scientia Iranica*. 2017; 25(4): 2087-97. DOI: 10.24200/sci.2017.4496.
 34. Zou X, Dong H, Qian SY. Influence of dynamic tissue properties on temperature elevation and lesions during HIFU scanning therapy: Numerical

- simulation. Chinese Physics B. 2020; 29(3):034305. DOI: 10.1088/1674-1056/ab6c4f.
35. Anneveldt KJ, van't Oever HJ, Verpalen IM, Nijholt IM, Bartels W, Dijkstra JR, et al. Increased MR-guided high intensity focused ultrasound (MR-HIFU) sonication efficiency of uterine fibroids after carbetocin administration. *European Journal of Radiology Open.* 2022 Jan 1;9:100413. DOI:10.1016/j.ejro.2022.100413.
 36. Zhou Y, Cunitz BW, Dunmire B, Wang YN, Karl SG, Warren C, et al. Characterization and Ex Vivo evaluation of an extracorporeal high-intensity focused ultrasound (HIFU) system. *Journal of Applied Clinical Medical Physics.* 2021 Sep;22(9):345-59. 2021; 22(9): 345-59. DOI:10.1002/acm2.13074.
 37. Dong H, Xiao ZO, Qian S. Simulation study on the influence of temperature- dependent acoustic-thermal parameters on tissue lesion under HIFU irradiation. *University Politehnica of Bucharest Scientific Bulletin-Series A-Applied Mathematics and Physics.* 2020; 82(2):207-20.